AIP Advances

Solution-grown small-molecule organic semiconductor with enhanced crystal alignment and areal coverage for organic thin film transistors

Sheng Bi, Zhengran He, Jihua Chen, and Dawen Li

Citation: AIP Advances **5**, 077170 (2015); doi: 10.1063/1.4927577
View online: http://dx.doi.org/10.1063/1.4927577
View Table of Contents: http://scitation.aip.org/content/aip/journal/adva/5/7?ver=pdfcov
Published by the AIP Publishing

Solution-grown small-molecule organic semiconductor with enhanced crystal alignment and areal coverage for organic thin film transistors

Sheng Bi,[1] Zhengran He,[1] Jihua Chen,[2] and Dawen Li[1,a]
[1]*Department of Electrical and Computer Engineering, Center for Materials for Information Technology, The University of Alabama, Tuscaloosa, AL 35487, USA*
[2]*Center for Nanophase Materials Sciences, Oak Ridge National Laboratory, Oak Ridge, TN 37831, USA*

(Received 1 May 2015; accepted 15 July 2015; published online 24 July 2015)

Drop casting of small-molecule organic semiconductors typically forms crystals with random orientation and poor areal coverage, which leads to significant performance variations of organic thin-film transistors (OTFTs). In this study, we utilize the controlled evaporative self-assembly (CESA) method combined with binary solvent system to control the crystal growth. A small-molecule organic semiconductor, 2,5-Di-(2-ethylhexyl)-3,6-bis(5″-n-hexyl-2,2′,5′,2″]terthiophen-5-yl)-pyrrolo[3,4-c] pyrrole-1,4-dione (SMDPPEH), is used as an example to demonstrate the effectiveness of our approach. By optimizing the double solvent ratios, well-aligned SMDPPEH crystals with significantly improved areal coverage were achieved. As a result, the SMDPPEH based OTFTs exhibit a mobility of 1.6×10^{-2} cm^2/Vs, which is the highest mobility from SMDPPEH ever reported. [http://dx.doi.org/10.1063/1.4927577]

I. INTRODUCTION

Solution processable small-molecule organic semiconductors have been intensively studied nowadays due to their relatively high charge carrier transport,[1–4] and cost-effectiveness in fabrication, which make them promising for applications in flexible electronics over large areas.[5–7] However, thin films drop casted from small-molecule organic semiconductors typically exhibit random crystal orientation with poor coverage, which leads to significant performance variations of organic thin-film transistors (OTFTs).[8,9] Therefore, it is mandatory to well align the crystals in order to achieve performance consistency of OTFTs. Various efforts have been made to address these issues in different semiconducting material systems.[10–12] For example, Lee *et al*. demonstrated the growth of 6,13-bis(triisopropylsilylethynyl)pentacene (TIPS pentacene) on a slightly tilted substrate, resulting in an array of ribbon-shaped TIPS pentacene crystals well-aligned in the tilted direction of the substrate.[13] More recently, Li *et al*. employed a "droplet-pinned crystallization" method to control the crystal growth of C_{60}, which successfully leads to well-aligned C_{60} single crystals.[14] Nevertheless, the films obtained in all these work above still show low areal coverage, which must be improved in order to fabricate high-mobility OTFTs with performance uniformity.

In this work, we combine the "controlled evaporative self-assembly (CESA)" method[15–17] with double solvent scheme[18,19] to both control the crystal growth and enhance areal coverage of organic semiconductors. Since diketopyrrolopyrrole (DPP) based organic materials have attracted enormous interests for applications in both organic photovoltaics (OPV) and OTFTs, a derivative of DPP, 2,5-Di-(2-ethylhexyl)-3,6-bis(5″-n-hexyl-2,2′,5′,2″]terthiophen-5-yl)-pyrrolo[3,4-c] pyrrole-1,4-dione (SMDPPEH),[20–27] is used as an example to demonstrate the effectiveness of our

[a]Author to whom correspondence should be addressed. Email: dawenl@eng.ua.edu Phone number: (205)348-9930 Fax number: (205)348-6959

approach. When drop casted from single solvent (chloroform), SMDPPEH formed crystals with significant misorientation and poor film coverage. In comparison, the application of CESA method combined with double solvent system leads to greatly enhanced crystal alignment, film coverage and crystal width. As a result, the SMDPPEH OTFTs based on CESA approach and double solvent system exhibit a mobility of up to 1.6×10^{-2} cm^2/Vs. To the best of our knowledge, this is the highest mobility from SMDPPEH ever reported.

II. EXPERIMENT

SMDPPEH material was purchased from Sigma Aldrich and used as received. Bottom-gate, bottom-contact transistors were fabricated on heavily doped *n*-type silicon substrates with a 100 nm thickness of thermally grown SiO_2 layer. The gold electrodes were patterned by using standard photolithography followed by metal deposition and lift-off. The patterned substrates with Au source/drain contacts were cleaned by acetone and isopropyl alcohol sequentially. Then surface treatments, including hexamethyldisilazane (HMDS) and pentafluorobenzenethiol (PFBT) treatments, were carried out. HMDS treatment was utilized to passivate the silanol groups on the hydrophilic SiO_2 substrate surface, whereas PFBT treatment was performed to tune the energy level of gold contacts for facilitating hole charge injection.[28] Specifically, HMDS self-assembled monolayers were formed on the gate dielectric via vapor deposition at 140 °C, and rinsed off the residue of HMDS by isopropyl alcohol. PFBT treatment was performed on the source/drain gold contacts by immersing the substrates in a 10mM PFBT/toluene solution for 2 hours, followed by rinsing with toluene.

SMDPPEH in chloroform/ethanol double solvents (3 mg/ml) was drop casted onto the substrate to form an active layer. In the double solvent system, chloroform was selected as the "good" solvent since SMDPPEH can be well dissolved in chloroform, whereas ethanol was used as the "bad" solvent because of the limited solubility of SMDPPEH in ethanol. Moreover, the similarity of the boiling points between ethanol (78.4°C) and chloroform (61.2°C) ensures simultaneous evaporation when the CESA method is applied for crystal alignment. If there exists a big difference in boiling point between "good" and "bad" solvent, the solution will eventually ends up with one single solvent situation. Optical micrographs of SMDPPEH thin film were taken by using a Zeiss Axioplan optical microscope with a build-in camera. Current-voltage ($I - V$) characteristics were carried out with an Agilent B1500A semiconductor parameter analyzer. Each device was measured three times to ensure the consistency of results. All measurements were performed in ambient environment at room temperature. Field-effect mobilities in the saturation regime were extracted from the slope of the $(I_{DS})^{1/2} - V_{GS}$ transfer characteristic.

III. RESULTS AND DISCUSSION

DPP is best known for its ease of side-chain substitution which forms different functional groups and leads to a good field-effect mobility.[29–31] As a newly-developed derivative of DPP, SMDPPEH hosts two pendant alkyl chains, which increases its solubility and thermal stability.[32] The molecular structure of SMDPPEH is shown in Figure 1(a). When SMDPPEH is drop casted from single chloroform solvent, a few scattered crystals are formed on the substrate with random orientation and poor areal coverage (Figure 1(b)), while drop casted from chloroform/ethanol double solvents, the resultant films exhibit enhanced crystal density as shown in the optical images of Figure 1(c), because the "bad" solvent ethanol increases nucleation seeds for SMDPPEH crystallization. In both cases of crystal growth in single and double solvents, however, there is no uniform crystal orientation, which could cause significant device performance variation if such films are used as the active layer of OTFTs.[33,34] In order to address these issues, we applied the CESA method combined with the double solvent system to effectively control the crystallization, and obtained SMDPPEH crystalline films with enhanced crystal alignment and areal coverage.

The CESA method applied to effectively align the SMDPPEH crystals is illustrated in Figure 2(a). As shown in the schematic, SMDPPEH solution was constrained in the cylinder-on-flat

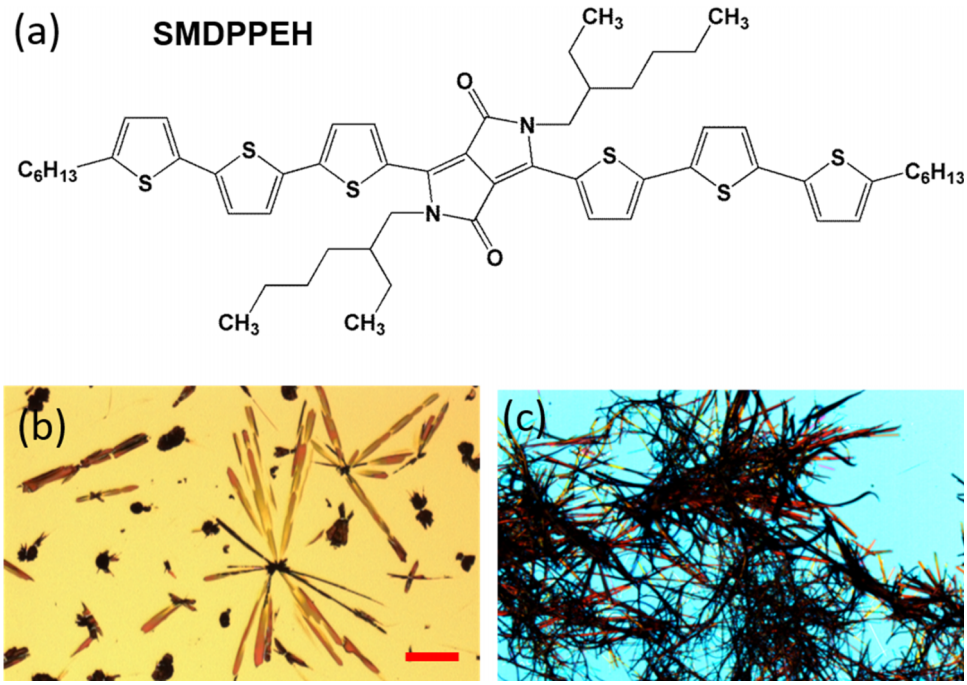

FIG. 1. (a) Molecular structure of SMDPPEH. Optical image of SMDPPEH crystals drop casted in (b) single chloroform solvent and (c) chloroform/ethanol (5:1) double solvents. Figure (b) and (c) share the same scale bar of 100 μm.

geometry, due to the capillary force between the cylinder and the substrate. When the contact line of the solution is pinned during solvent evaporation, the edge of the droplet has a higher evaporation rate which leads to elevated solution concentration.[35] This further facilitates an outward flow carrying more solutes from the droplet center to the periphery,[36] where nucleation seeds are formed from the solutes. When the solution reaches supersaturation, SMDPPEH molecules start to crystallize from the nucleation seeds and grow along the direction of capillary force towards the contact center between the cylinder and the substrate. With the combination of CESA method and double solvent system, well-aligned SMDPPEH crystals with significantly improved film coverage were achieved, as shown in the optical images of Figure 2(b). The digital image of Figure 2(c) shows the crystal growth over the entire substrate. The chloroform/ethanol double solvent is at 5:1 ratio.

In order to optimize the SMDPPEH film morphology with CESA method, different ratios between "good" solvent chloroform and "bad" solvent ethanol were tested. When a small amount of ethanol was added as in the case of chloroform/ethanol at 15:1 ratio, a few SMDPPEH crystals with enhanced crystal width and orientation were formed because only a small number of nucleation seeds from "bad" solvent ethanol were generated at this ratio, whereas the majority of the SMDPPEH material directly precipitated or formed many small crystals onto the substrate as round-shaped crystal aggregations as shown in Figure 3(a). When the amount of ethanol increased to chloroform/ethanol ratio of 10:1 and 5:1, both crystal orientation and coverage of the SMDPPEH film were improved (Figure 3(b) and 3(c)). Particularly, chloroform/ethanol at 5:1 ratio leads to the most improvement in the thin-film morphology of SMDPPEH, in terms of the best crystal alignment, the highest film coverage and the largest crystal width. However, if the amount of ethanol further increased to 1:1 (Figure 3(d)), both crystal width and film coverage of the SMDPPEH film decreased dramatically and crystal misorientation started to appear. Finally, the CESA method lost control of SMDPPEH crystal alignment when the amount of ethanol increased to chloroform/ethanol at 1:5 ratio, and the resultant film exhibited significant crystal misorientation with large gaps in between (Figure 3(e)).

The change in the crystal orientation, areal coverage and crystal width of the SMDPPEH film can be reasonably explained by the intermolecular interaction between SMDPPEH and ethanol.

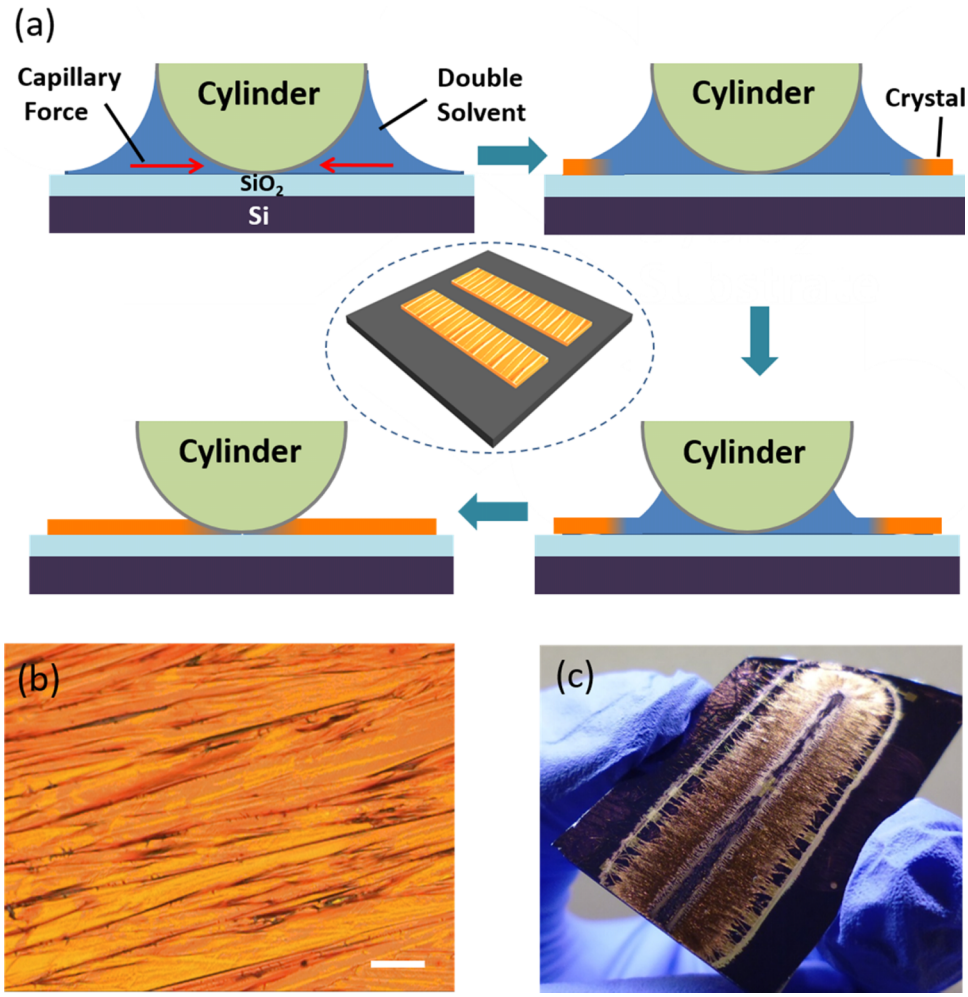

FIG. 2. (a) Schematic of the CESA method for crystal alignment. (b) The zoom in optical image of SMDPPEH films with highly orientated crystals and great film coverage. The scale bar represents 50 μm. (c) digital image of crystal growth over entire substrate with chloroform/ethanol ratio of 5:1.

When the ethanol solvent is added, it is expected that the hydroxyl groups in ethanol facilitate the intermolecular π-π overlapping of SMDPPEH backbones, further leading to the supramolecular aggregation of SMDPPEH molecules that serve as nucleation seeds.[37] When the solution supersaturation point is reached, the SMDPPEH molecules start to crystallize from the nucleation seeds and grow in the same direction as of the capillary force, resulting in well-aligned SMDPPEH crystals with enhanced crystal coverage and width. In specific, when a small amount of ethanol is added as in the case of chloroform and ethanol at 15:1 ratio, the slight supramolecular aggregation of SMDPPEH molecules created only a small number of nucleation seeds, contributing to the formation of a few well-aligned crystals, as illustrated in the top left cartoon of Figure 3(f). Nevertheless, the majority of the SMDPPEH material directly precipitated or formed many small crystals onto the substrate as round-shaped aggregations. When the ratio between chloroform and ethanol changes to 10:1 and 5:1, more addition of ethanol provided more hydroxyl groups and simultaneously increased both the nucleation seed number and density, which significantly enhances crystal width and film areal coverage while at the same time further improving the crystal alignment as illustrated in the bottom right cartoon of Figure 3(f). However, when the ratios between chloroform and ethanol further change to 1:1 and 1:5, it is likely that the excessive amount of ethanol would consume most of the SMDPPEH for the formation of nucleation seeds, so very few SMDPPEH solutes were dissolved in the solution as supply for crystallization, consequently leading to the

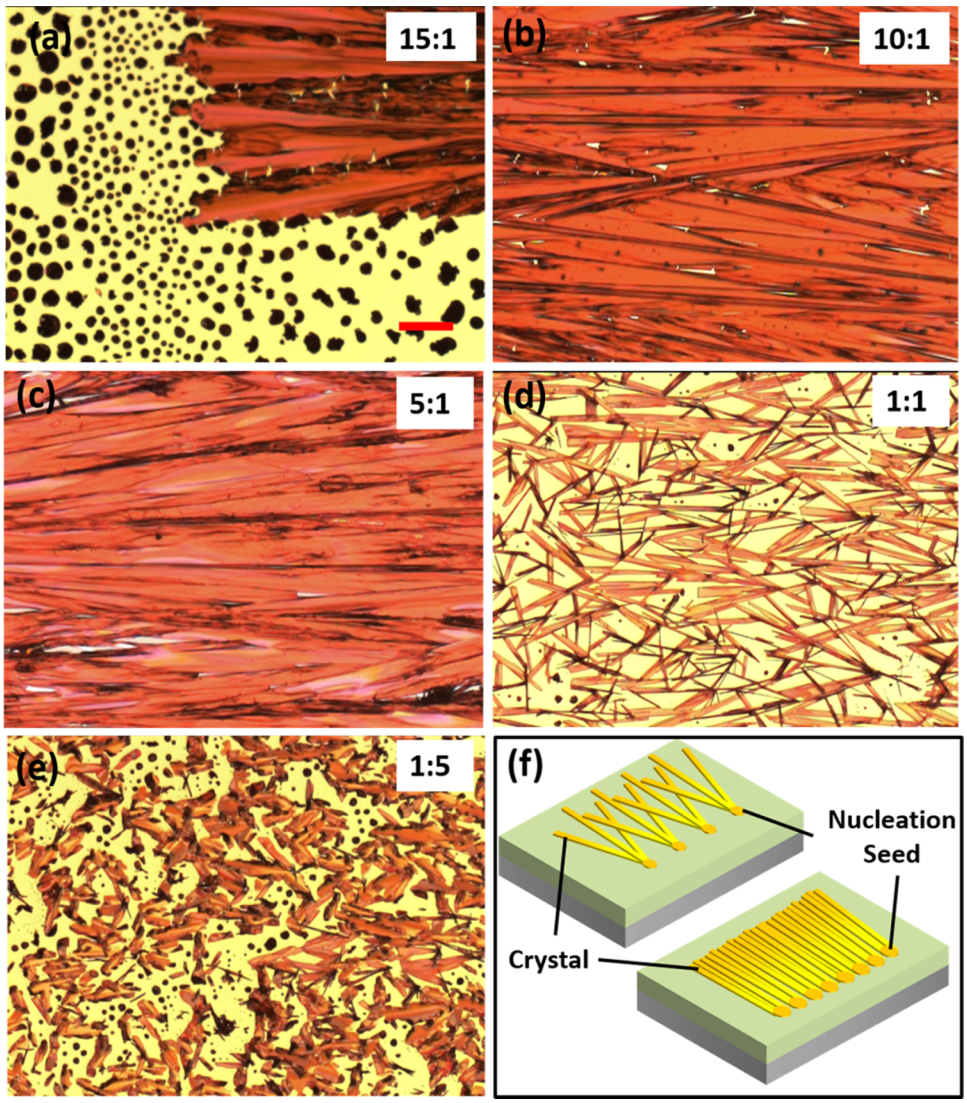

FIG. 3. Optical micrographs of SMDPPEH crystals drop casted from chloroform/ethanol double solvents at different ratios: (a) 15:1, (b) 10:1, (c) 5:1, (d) 1:1 and (e) 1:5, respectively. All images share the same scale bar of 100μm as shown in (a). (f) Effect of nucleation seed density on crystallization.

formation of many small crystals with significantly reduced crystal width, areal coverage and crystal orientation.

To more accurately demonstrate the effect of different double solvent ratios on the SMDPPEH thin film morphology, the average misorientation angle, crystal coverage and width were quantitatively characterized, as shown in Figure 4. The standard deviation of misorientation angle is based on 10 crystals for each type of film, whereas that of the crystal width is based on 14 crystals. The direction of capillary force is chosen as the baseline, and misorientation angle is defined as the angle between the long axis of a crystal ribbons and the baseline. The SMDPPEH film drop casted from chloroform/ethanol double solvent at the 15:1 ratio shows an average misorientation angle of $6 \pm 5°$, indicating the addition of a small amount of ethanol can largely reduce the crystal misorientation. The misorientation angle further reduces to $4 \pm 3°$ and $4 \pm 2°$ when the ethanol amount reaches to the 10:1 and 5:1 ratios, respectively, which demonstrates the SMDPPEH crystals are well-orientated. However, further increasing the ethanol amount to the 1:1 and 1:5 ratios would cause the misorientation angle to increase to $11 \pm 7°$ and $30 \pm 20°$, respectively.

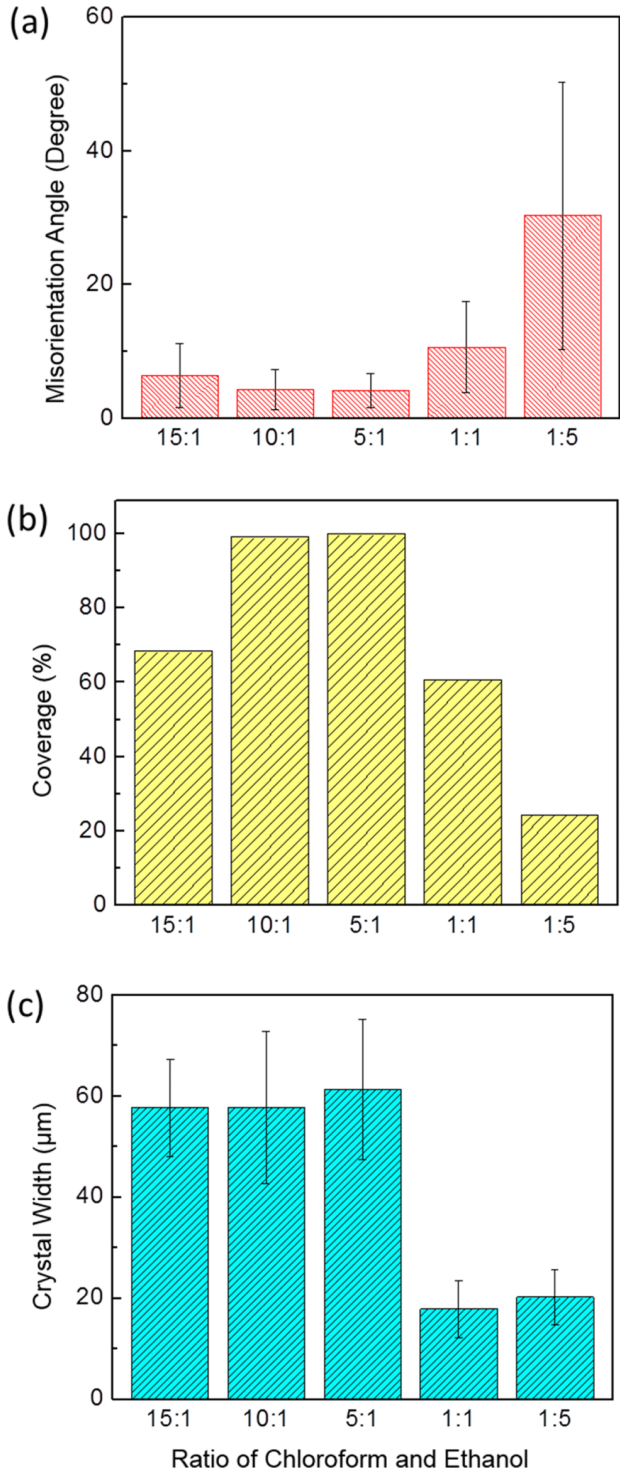

FIG. 4. Quantitative analysis of the (a) average crystal misorientation, (b) film coverage, and (c) average crystal width of the SMDPPEH crystals at different ratios of the chloroform/ethanol double solvents.

The areal coverage of the SMDPPEH films at different double solvent ratios was plotted in Figure 4(b). At chloroform/ethanol 15:1 ratio, the film has areal coverage of ~36%, which is enhanced to ~99% when the addition of ethanol increases to both 10:1 and 5:1 ratios, implying that the CESA method with optimal double solvent ratio can not only effectively align the crystal

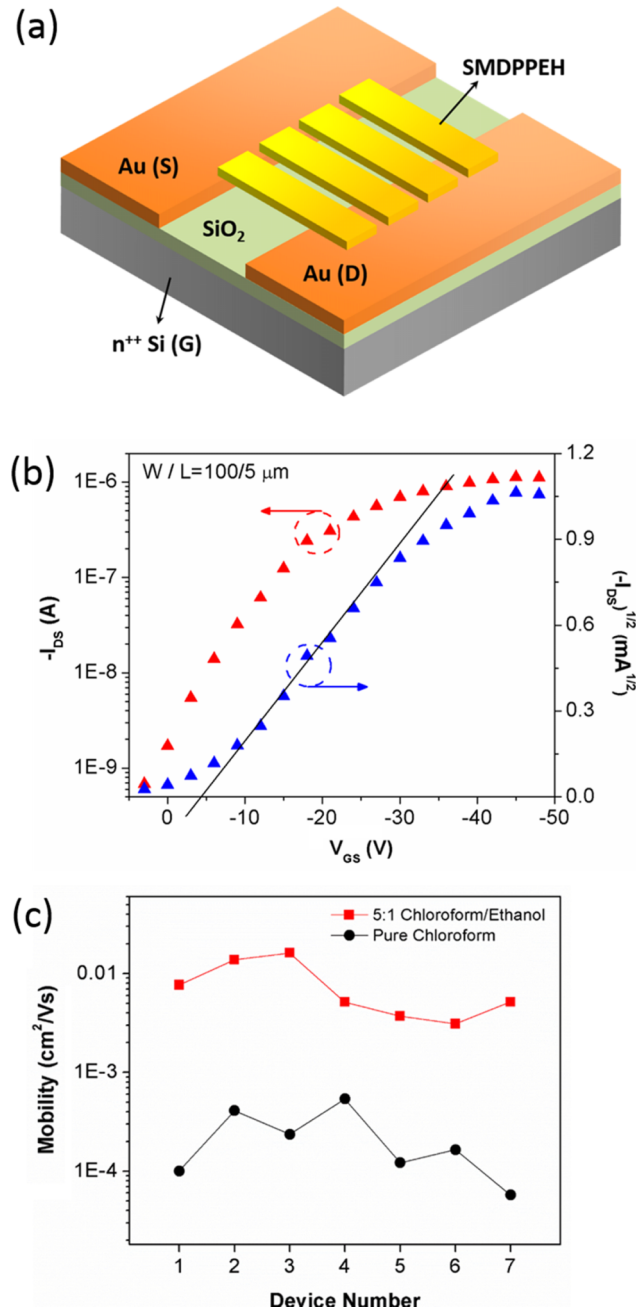

FIG. 5. (a) Schematic of bottom-gate, bottom-contact OTFTs with SMDPPEH crystal ribbons as active layer. (b) Transfer characteristics for field-effect mobility extraction. The volume ratio of chloroform to ethanol solvent is 5:1. (c) Mobility variation of SMDPPEH OTFTs based on different types of films.

growth, but also reduce the crystal gaps and enhance the film coverage. When the ethanol is further increased to 1:1 and 1:5 ratios, the areal coverage decreased to ~59% and ~57%, respectively. Moreover, the average crystal width of SMDPPEH films was also quantitatively calculated based on the optical microscope images and was plotted in Figure 4(c). The SMDPPEH film at chloroform/ethanol 15:1 ratio exhibits an average crystal width of 58 ± 10 μm, whereas those films at 10:1 and 5:1 ratios show an average crystal width of 58 ± 15 μm and 61 ± 14 μm, respectively. In particular, the chloroform/ethanol 5:1 leads to the largest crystal width. When the solvent volume ratio

further changes to 1:1 and 1:5, the average crystal width is reduced to 18 ± 6 μm and 20 ± 5 μm, respectively.

Bottom-gate, bottom-contact OTFTs were fabricated, and the device configuration with SMDPPEH microribbons as active semiconducting layer is illustrated in Figure 5(a). From the slope of the square root plot $(I_{DS})^{1/2} - V_{GS}$ in the transfer characteristic (Figure 5(b)), the field-effect mobility in the saturation region was extracted to be 1.6×10^{-2} cm^2/Vs by using the following traditional MOSFET equation:

$$I_{DS} = \left(\frac{WC_i\mu_{sat}}{2L}\right)(V_{GS} - V_T)^2 \quad (1)$$

where W is the effective channel width based on the actual crystal coverage in the channel region, L is the channel length, C_i is the capacitance per unit area of the gate insulator, μ_{sat} is the field-effect mobility in the saturated region, V_{GS} is the gate voltage and V_T is the threshold voltage. To the best of our knowledge, this is the highest mobility ever reported from the solution-processed SMDPPEH semiconductor. Moreover, our mobility is much larger than the value of other *p*-type semiconductors commonly studied as the donor materials of photovoltaic cells, such as poly(3-hexylthiophene-2,5-diyl) (P3HT),[38] indicating SMDPPEH is a promising donor material for solution-processed solar cells. In addition to the field-effect mobility, the threshold voltage V_T was extracted to be -4V, and the current on/off ratio $I_{on/off}$ is 4.3×10^4.

Finally, we plotted the OTFT mobilities against different types of films as shown in Figure 5(c). The mobilities of SMDPPEH OTFTs drop casted from pure chloroform without applying the CESA method varied from 5.7×10^{-5} cm^2/Vs to 5.4×10^{-4} cm^2/Vs, with an average mobility of $2.3 \times 10^{-4} \pm 1.8 \times 10^{-4}$ cm^2/Vs. In comparison, the devices made from 5:1 chloroform/ethanol double solvents with the CESA method demonstrated hole mobilities which ranged from 3.1×10^{-3} cm^2/Vs to 1.6×10^{-2} cm^2/Vs, with an average mobility of $7.8 \times 10^{-3} \pm 5.1 \times 10^{-3}$ cm^2/Vs. The results above demonstrated that the combination of CESA method and double solvent system effectively improves the charge transport and significantly enhances the average mobility of SMDPPEH OTFTs.

IV. CONCLUSIONS

In summary, we applied the CESA method combined with the double solvent system to achieve controlled crystallization of solution processable small-molecule organic semiconductors. SMDPPEH was used as an example to demonstrate the effectiveness of our approach. The greatly enhanced crystal alignment, film coverage and crystal width have been achieved. The effect of different ratios between the chloroform/ethanol double solvents on crystal film morphology were investigated, and chloroform/ethanol at 5:1 volume ratio was found to lead to the optimal film morphology with the best crystal orientation, the highest film coverage and the largest crystal width. As a result, a mobility of 1.6×10^{-2} cm^2/Vs has been obtained, which is the highest mobility from solution-processed SMDPPEH OTFTs ever reported.

ACKNOWLEDGMENTS

This work was supported by National Science Foundation (ECCS-1151140) and Research Stimulation Program at The University of Alabama. A portion of experimental design and analysis was conducted at the Center for Nanophase Materials Sciences, which is a DOE Office of Science User Facility.

[1] J. H. Chen, M. Shao, K. Xiao, Z. R. He, D. W. Li, B. S. Lokitz, D. K. Hensley, S. M. Kilbey, J. E. Anthony, J. K. Keum, A. J. Rondinone, W. Y. Lee, S. Y. Hong, and Z. A. Bao, "Conjugated Polymer-Mediated Polymorphism of a High Performance, Small-Molecule Organic Semiconductor with Tuned Intermolecular Interactions, Enhanced Long-Range Order, and Charge Transport," Chem. Mater. **25**, 4378 (2013).

[2] C. W. Sele, B. K. C. Kjellander, B. Niesen, M. J. Thornton, J. van der Putten, K. Myny, H. J. Wondergem, A. Moser, R. Resel, A. van Breemen, N. van Aerle, P. Heremans, J. E. Anthony, and G. H. Gelinck, "Controlled Deposition of Highly Ordered Soluble Acene Thin Films: Effect of Morphology and Crystal Orientation on Transistor Performance," Adv. Mater. **21**, 4926 (2009).

[3] Z. R. He, S. Shaik, S. Bi, J. H. Chen, and D. W. Li, "Air-stable solution-processed n-channel organic thin film transistors with polymer-enhanced morphology," Appl. Phys. Lett. **106**, 183301 (2015).
[4] R. Hamilton, J. Smith, S. Ogier, M. Heeney, J. E. Anthony, I. McCulloch, J. Veres, D. D. C. Bradley, and T. D. Anthopoulos, "High-Performance Polymer-Small Molecule Blend Organic Transistors," Adv. Mater. **21**, 1166 (2009).
[5] G. H. Gelinck, H. E. A. Huitema, E. Van Veenendaal, E. Cantatore, L. Schrijnemakers, J. Van der Putten, T. C. T. Geuns, M. Beenhakkers, J. B. Giesbers, B. H. Huisman, E. J. Meijer, E. M. Benito, F. J. Touwslager, A. W. Marsman, B. J. E. Van Rens, and D. M. De Leeuw, "Flexible active-matrix displays and shift registers based on solution-processed organic transistors," Nature Mater. **3**, 106 (2004).
[6] D. W. Li, E. J. Borkent, R. Nortrup, H. Moon, H. Katz, and Z. N. Bao, "Humidity effect on electrical performance of organic thin-film transistors," Appl. Phys. Lett. **86**, 042105 (2005).
[7] I. Bae, S. J. Kang, Y. J. Shin, Y. J. Park, R. H. Kim, F. Mathevet, and C. Park, "Tailored Single Crystals of Triisopropylsilylethynyl Pentacene by Selective Contact Evaporation Printing," Adv. Mater. **23**, 3398 (2011).
[8] Z. R. He, K. Xiao, W. Durant, D. K. Hensley, J. E. Anthony, K. L. Hong, S. M. Kilbey, J. H. Chen, and D. W. Li, "Enhanced Performance Consistency in Nanoparticle/TIPS Pentacene-Based Organic Thin Film Transistors," Adv. Func. Mater. **21**, 3617 (2011).
[9] Z. R. He, D. W. Li, D. K. Hensley, A. J. Rondinone, and J. H. Chen, "Switching phase separation mode by varying the hydrophobicity of polymer additives in solution-processed semiconducting small-molecule/polymer blends," Appl. Phys. Lett. **103**, 113301 (2013).
[10] K. Asare-Yeboah, R. M. Frazier, G. Szulczewski, and D. W. Li, "Temperature gradient approach to grow large, preferentially oriented 6,13-bis(triisopropylsilylethynyl) pentacene crystals for organic thin film transistors," J. Vac. Sci. Tech. B **32**, 052401 (2014).
[11] D. T. James, J. M. Frost, J. Wade, J. Nelson, and J. S. Kim, "Controlling Microstructure of Pentacene Derivatives by Solution Processing: Impact of Structural Anisotropy on Optoelectronic Properties," Acs Nano **7**, 7983 (2013).
[12] Z. R. He, N. Lopez, X. L. Chi, and D. W. Li, "Solution-based 5,6,11,12-tetrachlorotetracene crystal growth for high-performance organic thin film transistors," Org. Electron. **22**, 191 (2015).
[13] W. H. Lee, D. H. Kim, Y. Jang, J. H. Cho, M. Hwang, Y. D. Park, Y. H. Kim, J. I. Han, and K. Cho, "Solution-processable pentacene microcrystal arrays for high performance organic field-effect transistors," Appl. Phys. Lett. **90**, 132106 (2007).
[14] H. Y. Li, B. C. K. Tee, J. J. Cha, Y. Cui, J. W. Chung, S. Y. Lee, and Z. N. Bao, "High-Mobility Field-Effect Transistors from Large-Area Solution-Grown Aligned C-60 Single Crystals," J. Am. Chem. Soc. **134**, 2760 (2012).
[15] W. Han, M. Byun, L. Zhao, J. Rzayev, and Z. Lin, "Controlled evaporative self-assembly of hierarchically structured bottlebrush block copolymer with nanochannels," J. Mater. Chem. **21**, 14248 (2011).
[16] S. W. Kwon, M. Byun, D. H. Yoon, J.-H. Park, W.-K. Kim, Z. Lin, and W. S. Yang, "Simple route to ridge optical waveguide fabricated via controlled evaporative self-assembly," J. Mater. Chem. **21**, 5230 (2011).
[17] W. Han and Z. Q. Lin, "Learning from "Coffee Rings": Ordered Structures Enabled by Controlled Evaporative Self-Assembly," Angew. Chem. Int. Ed. **51**, 1534 (2012).
[18] D. H. Kim, D. Y. Lee, H. S. Lee, W. H. Lee, Y. H. Kim, J. I. Han, and K. Cho, "High-mobility organic transistors based on single-crystalline microribbons of triisopropylisilylethynl pentacene via solution-phase self-assembly," Adv. Mater. **19**, 678 (2007).
[19] H. Minemawari, T. Yamada, and T. Hasegawa, "Crystalline film growth of TIPS-pentacene by double-shot inkjet printing technique," Japan. J. Appl. Phys. **53** (2014).
[20] G. Q. Zhang, K. Liu, Y. Li, and M. J. Yang, "Novel poly(phenylene ethynylene)-type conjugated polymers containing diketopyrrolopyrrole or triphenylpyrazoline units in the main chain: Synthesis, characterization and photophysical properties," Poly. Intern. **58**, 665 (2009).
[21] M. Akita, I. Osaka, and K. Takimiya, "Quinacridone-Diketopyrrolopyrrole-Based Polymers for Organic Field-Effect Transistors," Materials **6**, 1061 (2013).
[22] M. J. Cho, J. Shin, S. H. Yoon, T. W. Lee, M. Kaur, and D. H. Choi, "A high-mobility terselenophene and diketopyrrolopyrrole containing copolymer in solution-processed thin film transistors," Chem. Comm. **49**, 7132 (2013).
[23] L. T. Dou, J. Gao, E. Richard, J. B. You, C. C. Chen, K. C. Cha, Y. J. He, G. Li, and Y. Yang, "Systematic Investigation of Benzodithiophene- and Diketopyrrolopyrrole-Based Low-Bandgap Polymers Designed for Single Junction and Tandem Polymer Solar Cells," J. Am. Chem. Soc. **134**, 10071 (2012).
[24] J. Ajuria, S. Chavhan, R. Tena-Zaera, J. H. Chen, A. J. Rondinone, P. Sonar, A. Dodabalapur, and R. Pacios, "Nanomorphology influence on the light conversion mechanisms in highly efficient diketopyrrolopyrrole based organic solar cells," Org. Elect. **14**, 326 (2013).
[25] J. W. Lee, Y. S. Choi, and W. H. Jo, "Diketopyrrolopyrrole-based small molecules with simple structure for high V-OC organic photovoltaics," Organic Electronics **13**, 3060 (2012).
[26] S. Y. Qu and H. Tian, "Diketopyrrolopyrrole (DPP)-based materials for organic photovoltaics," Chem. Comm. **48**, 3039 (2012).
[27] A. B. Tamayo, X.-D. Dang, B. Walker, J. Seo, T. Kent, and T.-Q. Nguyen, "A low band gap, solution processable oligothiophene with a dialkylated diketopyrrolopyrrole chromophore for use in bulk heterojunction solar cells," Appl. Phys. Lett. **94** (2009).
[28] K. Sakamoto, J. Ueno, K. Bulgarevich, and K. Miki, "Anisotropic charge transport and contact resistance of 6,13-bis(triisopropylsilylethynyl) pentacene field-effect transistors fabricated by a modified flow-coating method," Appl. Phys. Lett. **100** (2012).
[29] Y. Li, S. P. Singh, and P. Sonar, "A High Mobility P-Type DPP-Thieno 3,2-b thiophene Copolymer for Organic Thin-Film Transistors," Adv. Mater. **22**, 4862 (2010).
[30] A. D. Hendsbee, J.-P. Sun, L. R. Rutledge, I. G. Hill, and G. C. Welch, "Electron deficient diketopyrrolopyrrole dyes for organic electronics: synthesis by direct arylation, optoelectronic characterization, and charge carrier mobility," J. Mater. Chemi. A **2**, 4198 (2014).

[31] C. Kanimozhi, N. Yaacobi-Gross, E. K. Burnett, A. L. Briseno, T. D. Anthopoulos, U. Salzner, and S. Patil, "Use of side-chain for rational design of n-type diketopyrrolopyrrole-based conjugated polymers: what did we find out?," Phys. Chem. Chem. Phys. **16**, 17253 (2014).
[32] J. S. Zambounis, Z. Hao, and A. Iqbal, "Latent pigments activated by heat," Nature **388**, 131 (1997).
[33] Z. R. He, J. H. Chen, J. K. Keum, G. Szulczewski, and D. W. Li, "Improving performance of TIPS pentacene-based organic thin film transistors with small-molecule additives," Org. Electron. **15**, 150 (2014).
[34] Z. R. He, J. H. Chen, Z. Z. Sun, G. Szulczewski, and D. W. Li, "Air-flow navigated crystal growth for TIPS pentacene-based organic thin-film transistors," Org. Electron. **13**, 1819 (2012).
[35] R. D. Deegan, O. Bakajin, T. F. Dupont, G. Huber, S. R. Nagel, and T. A. Witten, "Capillary flow as the cause of ring stains from dried liquid drops," Nature **389**, 827 (1997).
[36] R. D. Deegan, O. Bakajin, T. F. Dupont, G. Huber, S. R. Nagel, and T. A. Witten, "Contact line deposits in an evaporating drop," Phys. Rev. E **62**, 756 (2000).
[37] X. R. Li, B. K. C. Kjellander, J. E. Anthony, C. W. M. Bastiaansen, D. J. Broer, and G. H. Gelinck, "Azeotropic Binary Solvent Mixtures for Preparation of Organic Single Crystals," Adv. Func. Mater. **19**, 3610 (2009).
[38] M. Kobashi and H. Takeuchi, "Inhomogeneity of spin-coated and cast non-regioregular poly(3-hexylthiophene) films. Structures and electrical and photophysical properties," Macromolecules **31**, 7273 (1998).